REPORT DOCUMENTATION PAGE

Form Approved OMB NO. 0704-0188

1. REPORT DATE (DD-MM-YYYY)	2. REPORT TYPE	3. DATES COVERED (From - To)
03-05-2015	Final Report	4-Sep-2009 - 3-Sep-2014

4. TITLE AND SUBTITLE

Final Report: Ultracold Molecules in Optical Lattices:Efficient Production And Application to Molecular Clocks

5a. CONTRACT NUMBER
W911NF-09-1-0504

5b. GRANT NUMBER

5c. PROGRAM ELEMENT NUMBER
611103

6. AUTHORS
Tanya Zelevinsky

5d. PROJECT NUMBER

5e. TASK NUMBER

5f. WORK UNIT NUMBER

7. PERFORMING ORGANIZATION NAMES AND ADDRESSES
Columbia University
615 W. 131st St.
Room 254, MC 8725
New York, NY 10027 -7922

8. PERFORMING ORGANIZATION REPORT NUMBER

9. SPONSORING/MONITORING AGENCY NAME(S) AND ADDRESS (ES)

U.S. Army Research Office
P.O. Box 12211
Research Triangle Park, NC 27709-2211

10. SPONSOR/MONITOR'S ACRONYM(S)
ARO

11. SPONSOR/MONITOR'S REPORT NUMBER(S)
54728-PH-PCS.13

12. DISTRIBUTION AVAILIBILITY STATEMENT

Approved for Public Release; Distribution Unlimited

13. SUPPLEMENTARY NOTES

The views, opinions and/or findings contained in this report are those of the author(s) and should not contrued as an official Department of the Army position, policy or decision, unless so designated by other documentation.

14. ABSTRACT

We have established the strontium molecular clock as the leading ultracold-molecule precision measurement platform. We can fully control the molecules' internal and external quantum states, as in state-of-the-art atomic lattice clocks. Using the quantized molecular spectra in an optical lattice, we devised a new lattice thermometry method that is advantageous for many lattice experiments, including clocks and many-body physics studies. The full quantum control allowed us to observe deeply subradiant molecular states, and coherently control them. We measured lifetimes enhanced by up to 200 times. Ultranarrow transitions to these states permitted a rigorous study

15. SUBJECT TERMS

Laser cooling, ultracold molecules, lattice clocks, high-resolution spectroscopy

16. SECURITY CLASSIFICATION OF:			17. LIMITATION OF ABSTRACT	15. NUMBER OF PAGES	19a. NAME OF RESPONSIBLE PERSON
a. REPORT	b. ABSTRACT	c. THIS PAGE			Tanya Zelevinsky
UU	UU	UU	UU		19b. TELEPHONE NUMBER 212-851-0767

Report Title

Final Report: Ultracold Molecules in Optical Lattices:Efficient Production And Application to Molecular Clocks

ABSTRACT

We have established the strontium molecular clock as the leading ultracold-molecule precision measurement platform. We can fully control the molecules' internal and external quantum states, as in state-of-the-art atomic lattice clocks. Using the quantized molecular spectra in an optical lattice, we devised a new lattice thermometry method that is advantageous for many lattice experiments, including clocks and many-body physics studies. The full quantum control allowed us to observe deeply subradiant molecular states, and coherently control them. We measured lifetimes enhanced by up to 300 times. Ultranarrow transitions to these states permitted a rigorous study of asymptotic physics at the atom-molecule threshold. We proved that subradiant states can decay to the ground state via higher-order electromagnetic transitions, with a rate that grows as the square of the bond length, and are quenched by predissociation at a rate proportional to the vibrational level spacing. We introduced a precise technique for measuring molecular binding energies via photofragmentation; controlled forbidden optical transition strengths with weak magnetic fields by five orders of magnitude; and explained anomalously large magnetic susceptibilities of the asymptotic molecules. The unprecedented precision, coupled with advanced ab initio theory, paves the way to exciting new directions for the molecular clock.

Enter List of papers submitted or published that acknowledge ARO support from the start of the project to the date of this printing. List the papers, including journal references, in the following categories:

(a) Papers published in peer-reviewed journals (N/A for none)

Received		Paper
05/03/2015	7.00	C. B. Osborn, B. H. McGuyer, M. McDonald, G. Reinaudi, W. Skomorowski, R. Moszynski, T. Zelevinsky. Nonadiabatic Effects in Ultracold Molecules via Anomalous Linear and Quadratic Zeeman Shifts, Physical Review Letters, (12 2013): 0. doi: 10.1103/PhysRevLett.111.243003
05/03/2015	10.00	M. McDonald, B.?H. McGuyer, G.?Z. Iwata, T. Zelevinsky. Thermometry via Light Shifts in Optical Lattices, Physical Review Letters, (01 2015): 0. doi: 10.1103/PhysRevLett.114.023001
05/03/2015	9.00	B. H. McGuyer, M. McDonald, G. Z. Iwata, M. G. Tarallo, W. Skomorowski, R. Moszynski, T. Zelevinsky. Precise study of asymptotic physics with subradiant ultracold molecules, Nature Physics, (12 2014): 0. doi: 10.1038/nphys3182
05/03/2015	8.00	Mickey McDonald, Jiyoun Ha, Bart H. McGuyer, Tanya Zelevinsky. Visible optical beats at the hertz level, American Journal of Physics, (10 2014): 0. doi: 10.1119/1.4890502
08/15/2013	3.00	C. B. Osborn, G. Reinaudi, K. Bega, T. Zelevinsky. Dynamically configurable and optimizable Zeeman slower using permanent magnets and servomotors, Journal of Optical Society of America B, (03 2012): 729. doi:
08/15/2013	6.00	G. Reinaudi, C. B. Osborn, M. McDonald, S. Kotochigova, T. Zelevinsky. Optical Production of Stable Ultracold ^{88}Sr_{2} Molecules, Physical Review Letters, (09 2012): 115303. doi: 10.1103/PhysRevLett.109.115303
TOTAL:		**6**

Number of Papers published in peer-reviewed journals:

(b) Papers published in non-peer-reviewed journals (N/A for none)

Received Paper

TOTAL:

Number of Papers published in non peer-reviewed journals:

(c) Presentations

Presented results at 8 international conferences.

Number of Presentations: 8.00

Non Peer-Reviewed Conference Proceeding publications (other than abstracts):

Received Paper

TOTAL:

Number of Non Peer-Reviewed Conference Proceeding publications (other than abstracts):

Peer-Reviewed Conference Proceeding publications (other than abstracts):

Received Paper

TOTAL:

Number of Peer-Reviewed Conference Proceeding publications (other than abstracts):

(d) Manuscripts

Received		Paper
05/03/2015	11.00	Bart H. McGuyer, Mickey McDonald, Geoffrey Z. Iwata, W. Skomorowski, R. Moszynski, T. Zelevinsky. Control of Optical Transitions with Magnetic Fields in Weakly Bound Molecules, Physical Review Letters (submitted) (03 2015)
08/15/2013	5.00	B. H. McGuyer, C. B. Osborn, M. McDonald, G. Reinaudi, W. Skomorowski, R. Moszynski, T. Zelevinsky. Measurement of Nonadiabatic Effects in Ultracold Molecules via Anomalous Linear and Quadratic Zeeman Shifts, ArXiv e-prints (07 2013)
08/23/2012	2.00	G. Reinaudi, C. B. Osborn, M. McDonald, S. Kotochigova, T. Zelevinsky. Optical Production of Stable Ultracold 88Sr2 Molecules, Physical Review Letters (accepted) (06 2012)
TOTAL:		**3**

Number of Manuscripts:

Books

Received	Book
TOTAL:	

Received	Book Chapter
TOTAL:	

Patents Submitted

Patents Awarded

Awards

Sloan Research Fellowship, 2010
Kavli Frontiers Fellow, National Academy of Sciences
NIST Precision Measurement Grant, 2013
NSF CAREER Award, 2014

Graduate Students

NAME	PERCENT_SUPPORTED	Discipline
Christopher B. Osborn	0.50	
Mickey McDonald	0.05	
FTE Equivalent:	**0.55**	
Total Number:	**2**	

Names of Post Doctorates

NAME	PERCENT_SUPPORTED
Bart H. McGuyer	0.20
Gael Reinaudi	0.50
FTE Equivalent:	**0.70**
Total Number:	**2**

Names of Faculty Supported

NAME	PERCENT_SUPPORTED	National Academy Member
Tanya Zelevinsky	0.08	
FTE Equivalent:	**0.08**	
Total Number:	**1**	

Names of Under Graduate students supported

NAME	PERCENT_SUPPORTED	Discipline
Matthew Miecnikowski	0.00	Physics
Noel Wan	0.00	Physics
Dili Wang	0.00	Physics
Clio Sleator	0.00	Physics
Paul Lintilhac	0.00	Physics
Michael Rubin	0.00	Engineering
Siqing Yu	0.00	Physics
Raanan Cohen	0.00	Engineering
Paul Mueller	0.00	Engineering
David Tam	0.00	Physics
FTE Equivalent:	**0.00**	
Total Number:	**10**	

Student Metrics

This section only applies to graduating undergraduates supported by this agreement in this reporting period

The number of undergraduates funded by this agreement who graduated during this period: 7.00

The number of undergraduates funded by this agreement who graduated during this period with a degree in science, mathematics, engineering, or technology fields:..... 7.00

The number of undergraduates funded by your agreement who graduated during this period and will continue to pursue a graduate or Ph.D. degree in science, mathematics, engineering, or technology fields:..... 7.00

Number of graduating undergraduates who achieved a 3.5 GPA to 4.0 (4.0 max scale):..... 7.00

Number of graduating undergraduates funded by a DoD funded Center of Excellence grant for Education, Research and Engineering:..... 0.00

The number of undergraduates funded by your agreement who graduated during this period and intend to work for the Department of Defense 0.00

The number of undergraduates funded by your agreement who graduated during this period and will receive scholarships or fellowships for further studies in science, mathematics, engineering or technology fields: 0.00

Names of Personnel receiving masters degrees

NAME
Florian Apfelbeck
Camille Frapolli
Total Number: **2**

Names of personnel receiving PHDs

NAME
Christopher B. Osborn, 2013
Total Number: **1**

Names of other research staff

NAME	PERCENT_SUPPORTED
FTE Equivalent:	
Total Number:	

Sub Contractors (DD882)

Inventions (DD882)

Scientific Progress

See Attachment

Technology Transfer

1 Background

In this final PECASE project report, we describe the results of the molecular lattice clock experiment at Columbia University, particularly those achieved over the past year, and discuss the future outlook. This ARO award has enabled our laboratory to launch a highly successful experiment that has advanced the state of the art in molecular metrology, and serves as a starting point for many more precision measurements that have not been possible to date.

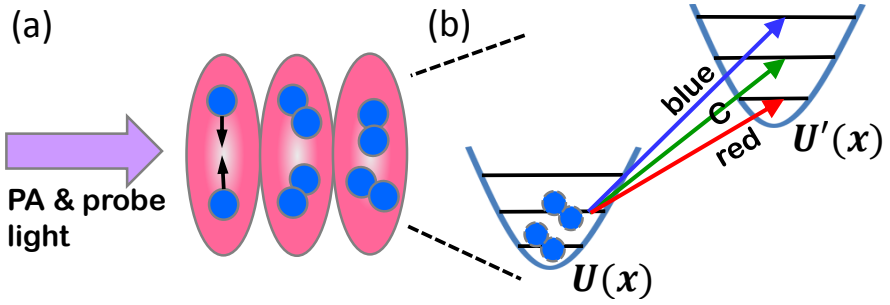

Figure 1: (a) ^{88}Sr atoms are trapped and cooled in a 1D optical lattice, and subsequently photoassociated on the narrow 689 nm intercombination line ($^1S_0 - {}^3P_1$) to create ultracold diatomic molecules. The molecules are then probed along the lattice axis in the Lamb-Dicke and resolved sideband regimes. (b) The carrier (C) and blue and red sideband transitions between long-lived electronic states in an approximately harmonic trap are indicated. Graphics from Ref. [1].

The molecular clock experiment constitutes a unique system yielding deep and precise understanding of molecular physics, quantum chemistry, precision metrology, and fundamental physics. At the heart of the experiment are creation and precise spectroscopy of ultracold alkaline-earth-metal atom dimers composed of two bosonic isotopes of strontium, $^{88}Sr_2$. The molecules are created, probed, and imaged in an optical lattice trap that provides a Lamb-Dicke and resolved sideband spectroscopy regime [2] that quantizes the motion and thus effectively removes Doppler shifts from the spectra. Figure 1 schematically illustrates molecule creation in the lattice and the spectroscopy approach that yields ultranarrow carrier spectra as well as red and blue sidebands. Thus, our experiment is a merging of the fields of ultracold molecular science [3] and atomic lattice clocks [4], resulting in a powerful tool for metrology and sensitivity to new physics.

This work has impacts on technology, science, and education. Atomic and molecular clocks have applications in geodesy, navigation, and tests of fundamental science. The skills and knowledge acquired by students who work on these projects are valued in many professions. We tackle education at all levels, and make our laboratory resources available to the students who otherwise might not have an opportunity to interact with cutting-edge technology.

2 Experimental challenges and solutions

The creation of $^{88}Sr_2$ molecule in an optical lattice was first described in Ref. [5]. In subsequent years, we have better understood and optimized the process, and tackled some outstanding major challenges.

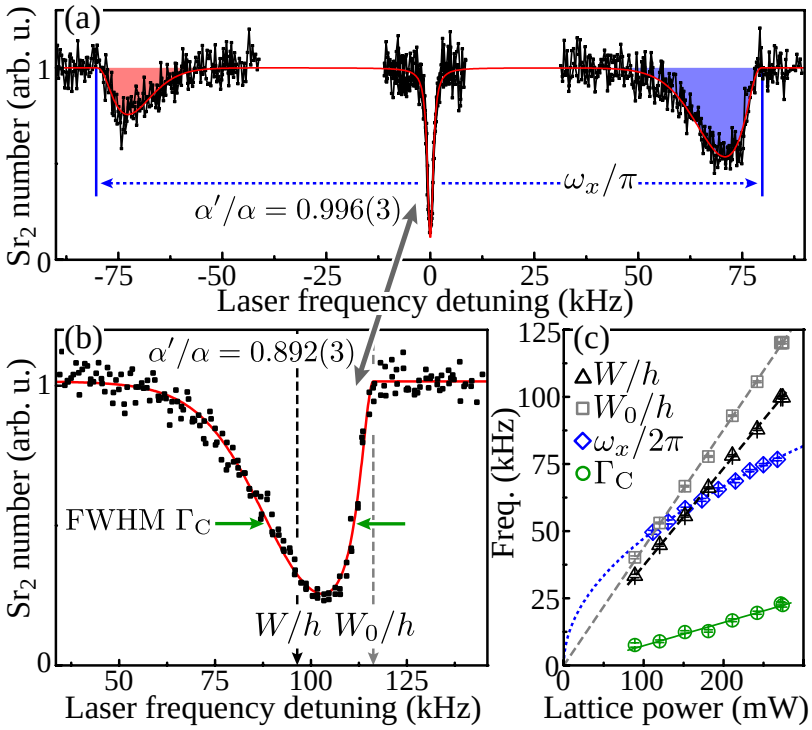

Figure 2: (a) An optical spectrum of Sr_2 molecules in a state-insensitive lattice (i.e. the polarizability ratio $\alpha'/\alpha \approx 1$). The central carrier transition and the first-order red and blue sidebands are visible. The axial trap frequency $f_x \sim 80$ kHz is found from the SB spacing, while the transverse (radial) trap frequency $f_r \sim 0.6$ kHz. (b) The carrier line shape in a state-sensitive lattice ($\alpha'/\alpha \approx 0.9$), including light-induced shift and broadening. The average light shift, W/h, and the temperature-independent contribution to the light shift, W_0/h, are indicated. Zero detuning of the probe laser on the horizontal axes in (a) and (b) corresponds to zero lattice light shift. (c) The dependence of W/h, W_0/h, f_x, and the FWHM Γ_C on the lattice light power. Graphics from Ref. [1].

For work with ultracold molecules in lattices, the lowest possible temperatures are desirable. In laser-cooled Sr gases, sub-μK temperatures are achieved directly with laser cooling. However, when diatomic molecules are formed via photoassociation [6], the temperature is expected to increase somewhat, due to incoherent photon scattering by the formed molecules. This resulting temperature is very difficult to measure, since traditional ultracold thermometry techniques fail if there are no optical cycling transitions, or if the particle number is low. One common method to measure ultracold atom temperature is via the time-of-flight imaging [7], but this method involves collecting an optical image of an expanding cloud, and does not work on molecules due to the lack of an efficiently cycling transition.

In addition, it is desirable to devise a thermometry technique that relies on spectroscopy rather than imaging, to enhance precision and accuracy. We invented such a technique, which is applicable to any lattice-trapped atom or molecule with a narrow spectral line, and should not break down even into the nanokelvin temperatures. It relies on highly precise spectral line shapes of carrier transitions in optical lattices. A sample spectrum is shown in Fig. 2(a), showing both the carrier and the sidebands at 'magic' optical lattice conditions [8]. Sideband spectra are commonly used for thermometry in optical lattice clocks [9], since temperature is directly related to the ratio of the blue-to-red sideband areas. However, this technique usually breaks down at temperatures below

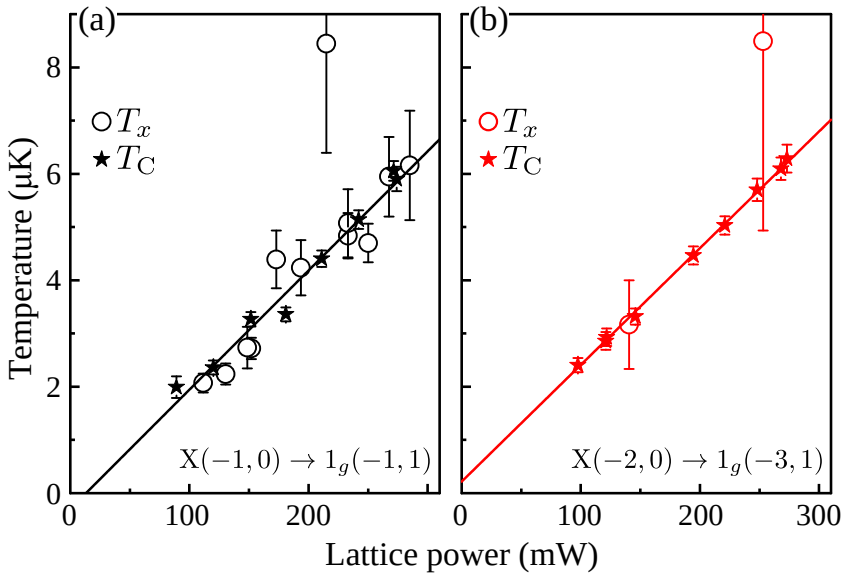

Figure 3: Carrier thermometry of ultracold molecules (stars) is compared with an alternative technique that uses sideband areas (circles), for (a) $v = -1$ and (b) $v = -2$ molecules. The notation (v, J) specifies the vibrational level and total angular momentum of the molecule. The molecular potentials X and 1_g [10] are separated by an optical frequency. Graphics from Ref. [1].

a microkelvin due to the vanishingly small red sideband area in that regime. Instead, the temperature can be mapped onto the carrier line shape, if the lattice conditions are not perfectly magic. Figure 2(b) shows the carrier when the excited-to-ground state polarizability ratio is ~ 0.9. We found that the position of the sharp corner is given by the differential light shift and is temperature-independent, while the total linewidth is proportional to the 3D temperature T [1], as shown in Fig. 2(c).

This technique proved nearly an order of magnitude more precise than the sideband ratio technique, as illustrated in Fig. 3. Moreover, the figure demonstrates that this technique is highly immune to a reduced signal-to-noise ratio due to a low particle number, as is the case in panel (b). Figure 4(a-c) shows how we successfully used the new 'carrier thermometry' technique to characterize heating processes in photoassociative molecule formation. Moreover, we demonstrated a 'carrier cooling' technique as in Fig. 4(d), somewhat analogous to well-known sideband cooling, but taking advantage of the carrier's high signal-to-noise ratio. The work on lattice thermometry is applicable not only to atomic and molecular lattice clocks, but to many experiments that use lattice-trapped atoms. It addresses a key problem on the interface between atomic and condensed matter physics research [11].

Another key challenge in molecular metrology is the question whether it is feasible to engineer magic, or state-insensitive, optical lattices for narrow molecular transitions, similarly to what is commonly done for atomic lattice clocks. We have solved this challenge for a number of narrow molecular transitions, particularly the ultrahigh-Q transitions that are electric-dipole forbidden by molecular parity considerations (Sec. 3). Figure 5 shows the tuning of the differential lattice light shift via the lattice polarization angle and wavelength. This has allowed us to reach molecular quality factors exceeding 10^{12} [10], an important prerequisite for precise molecular metrology.

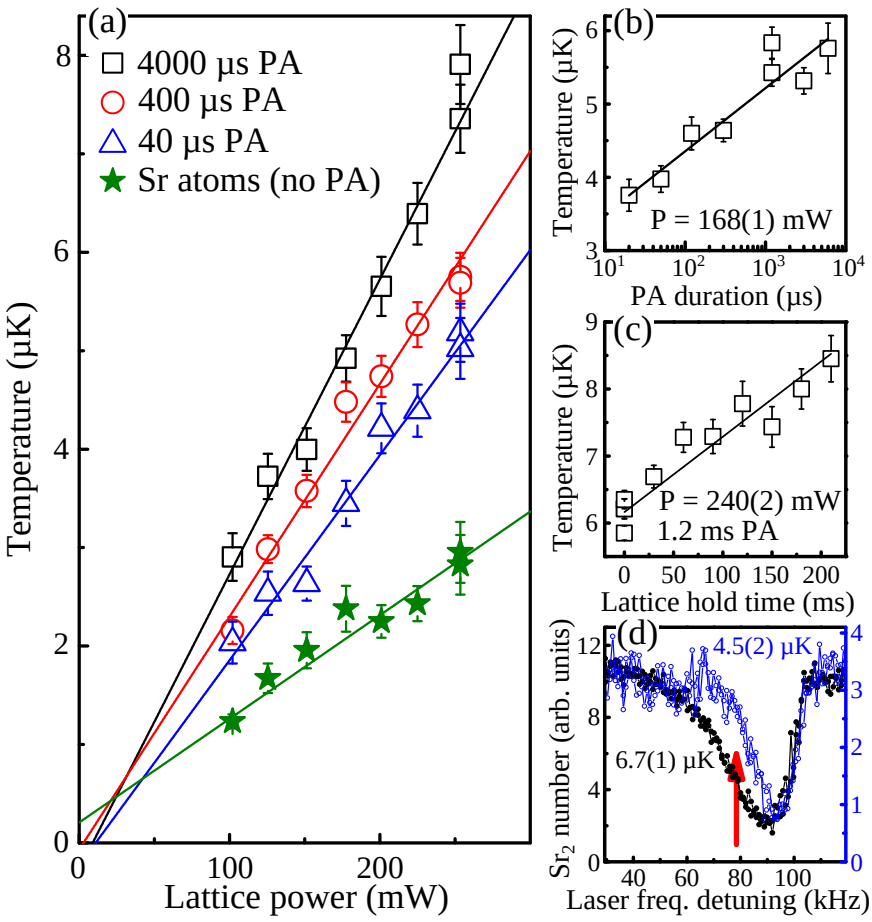

Figure 4: (a) Molecule temperatures at various lattice light powers via carrier thermometry, along with the initial atom temperatures via time-of-flight expansion imaging. (b) Molecule temperature versus the PA pulse duration. (c) Molecule temperature versus the lattice hold time. (d) Carrier cooling of molecules in a weakly state-sensitive lattice. Graphics from Ref. [1].

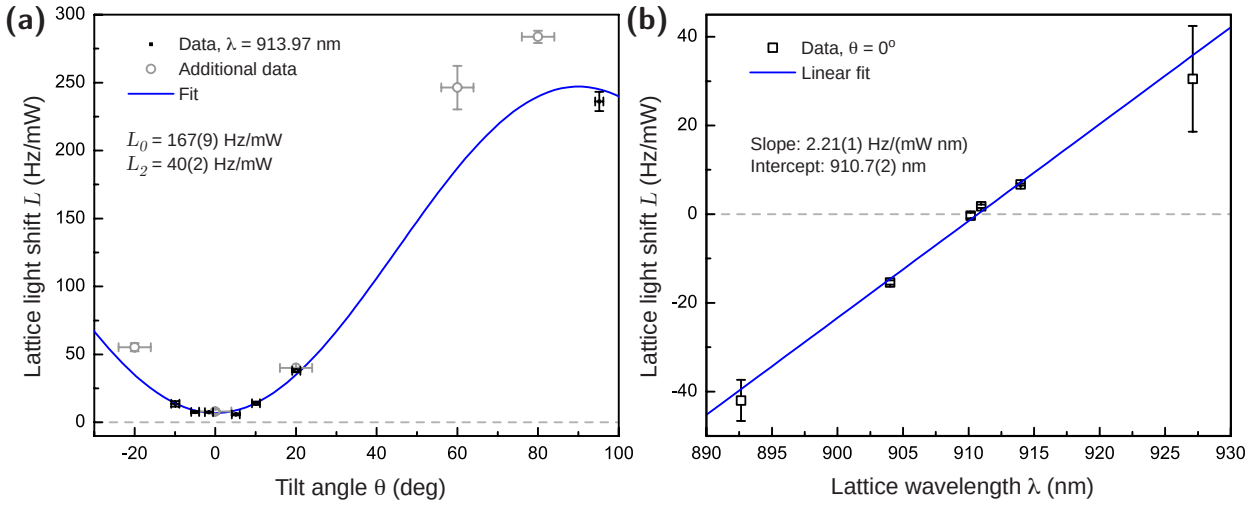

Figure 5: Polarization and wavelength tuning of the lattice light shift, for an electric-dipole forbidden optical transition. The probed transition is from $v = -2$, $J = 0$ of $X0_g^+$ to $v' = -4$, $J' = 1$ of 1_g [10]. (a) The shift is controlled by varying the lattice polarization direction relative to the quantum axis. (b) The shift is controlled by varying the lattice wavelength, at the optimal polarization determined from part (a). Graphics from Supplementary Information of Ref. [10].

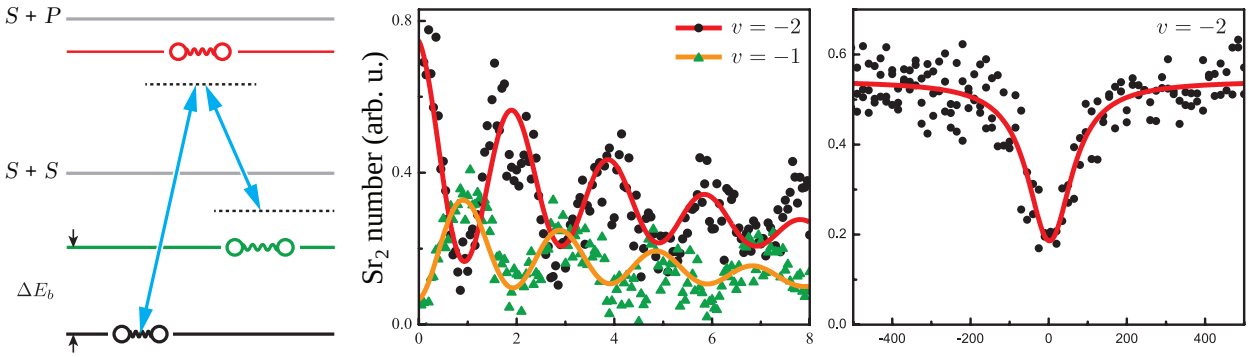

Figure 6: Two-color Raman transitions between vibrational levels of ground-state Sr_2 molecules. (a) Schematic energy level diagram. (b) The detected populations of the initial and final vibrational levels with $J = 0$ show coherent Rabi oscillations as a function of the Raman pulse length. (c) The linewidths of the Raman transitions are mostly limited by thermal decoherence from differential lattice light shifts [1]. For this trace, a Lorentzian fit to the natural logarithm of the data (to account for linear probe absorption) yields a 112(8) Hz FWHM. Graphics from Ref. [12].

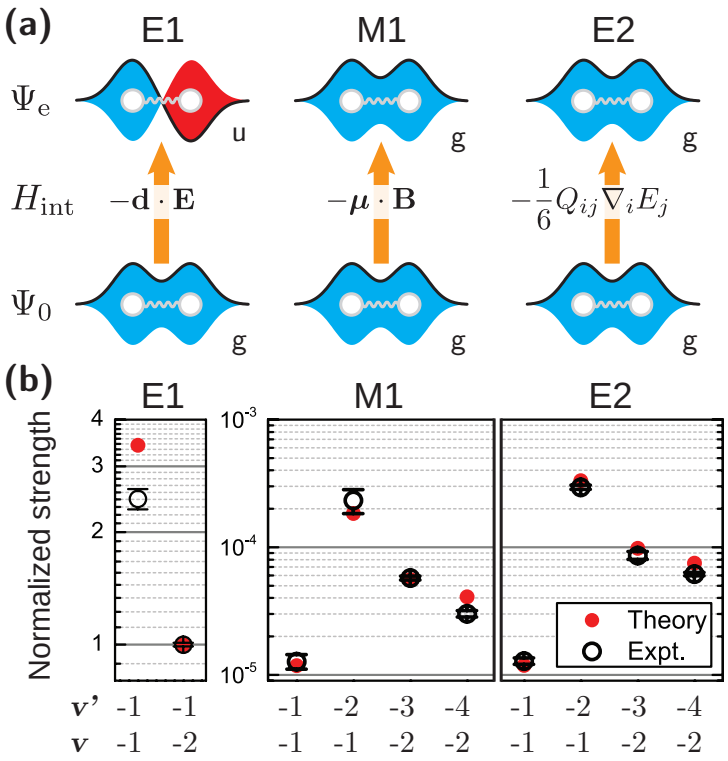

Figure 7: Optical transitions to superradiant and subradiant molecular states. (a) Electric dipole (E1), magnetic dipole (M1), and electric quadrupole (E2) transitions in homonuclear diatomic molecules, from the gerade ground state to ungerade or gerade excited states. (b) Measurements and predictions of E1, M1, and E2 transition oscillator strengths in the weakly bound $^{88}Sr_2$ molecule. All values are normalized to an E1 transition (to a 1_u level) with a nominal oscillator strength of unity. Graphics from Ref. [10].

Another challenge we have addressed is the possibility of coherent optical manipulation of molecules. Figure 6 shows the results of coherent two-photon transfer of molecules between vibrational levels in the ground electronic state [12]. Such transfer is key to a number of future experiments in time and frequency metrology and nanometer scale mass-dependent force studies (Sec. 6). Coherent optical control of molecules is further described in Sec. 3.

3 Subradiant molecular clock and asymptotic physics

While superradiance has been actively explored in various experimental systems [13], the related quantum optical effect of subradiance remains rarely seen, due to the inherently weak interaction with the environment [14, 15]. However, this quantum effect is present in the electronic states of homonuclear diatomic molecules that have the same parity (gerade/ungerade) as the electronic ground state. The challenge of observing and characterizing it lies in the ability to probe extremely narrow optical molecular transitions.

With our apparatus, we were able to surmount this challenge, and carry out the first quantitative study of subradiance [10]. We have applied this complete suppression of electric dipole (E1) optical transitions from the 1_g excited potential near the intercombination-line asymptote to the

$X^1\Sigma_g^+$ ground state of Sr_2. This has allowed us to observe highly forbidden magnetic dipole (M1) and electric quadrupole (E2) optical decay processes, as in Fig. 7(a). The corresponding decay rates are $\sim 10^4\times$ weaker than for E1, and thus cannot be seen with only partial subradiance. Moreover, the rates of these higher-order radiative processes have been predicted to scale with the bond length as R^2 [16], but this scaling has never been observed. Figure 7(b) shows precise transition strength measurements for some of the key forbidden transitions, which indeed exhibit relative strengths of $\sim 10^{-4}$. The measurements show excellent agreement with a state-of-the-art ab initio quantum chemistry model [17] that contains the correct scaling with R.

With the discovery of subradiant states in Sr_2, coherent control of molecules in the optical regime was achieved. Figure 8(a) shows Rabi oscillations between the gerade ground and excited electronic states. Such oscillations enable targeting the molecules with π-pulses, and utilizing variable wait times to probe the remaining population with lifetime studies, such as shown in Fig. 8(b-d). When the lifetimes are converted to line widths, the dashed red Lorentzian traces in Fig. 8(e-h) result. These 'in-the-dark' line shapes agree with direct spectroscopic traces obtained in the Lamb-Dicke lattice trapping regime and also shown in Fig. 8(e-h). The exception is the narrowest trace that is limited by the ~ 150 Hz laser width in direct spectroscopy. This experiment has reached a record molecule-light coherence time of ~ 6 ms, limited only by the intrinsic laser linewidth which can be improved with well-known technology [18].

As a result of accessing fully subradiant states of Sr_2 and achieving long molecule-light coherence times, we were able to study new aspects of asymptotic atom-molecule physics. Besides the higher-order radiative decay processes described above (M1 and E2), for the first time we have observed and quantified ultracold non-radiative decay, or gyroscopic predissociation. Figure 9(a) schematically illustrates the coupling of weakly bound molecular states near the $^1S_0 + ^3P_1$ threshold to the $^1S_0 + ^3P_0$ atomic continuum. This coupling occurs through state mixing at short range. Despite it being a short-range effect, we were able to describe it with long-range physics, and find a simple and intuitive scaling of this effect with the bond length. The predissociative linewidths were shown to be proportional to the vibrational energy spacings, and thus decrease toward the asymptote. Figure 9(b) shows the measured linewidths for the four most weakly bound subradiant states, as well as for a pair of superradiant states near the same threshold, for reference. As expected, the superradiant emission is enhanced by a factor of ~ 2 (with slight corrections due to molecular effects). In contrast, very deep subradiance is achieved, with the narrowest linewidth $\sim 300\times$ below that of free atoms. As shown, the widths due to M1 and E2 radiative decay (as measured, calculated, and illustrated in Fig. 7(b)) are too low to account for the observed widths. However, non-radiative decay fully explains the observations.

4 Magnetic field control of forbidden transitions

In this molecular clock experiment, we have investigated many types of forbidden transitions. Optical transitions to subradiant states were discussed in Sec. 3. In addition, we have explored enabling electric-dipole (E1) forbidden transitions with weak magnetic fields, as schematically shown in Fig. 10. In the absence of field, only $\Delta J = 0, \pm 1$ are E1 allowed. Field-induced admixing of neighboring excited rotational levels has led to our observations of $\Delta J > 1$ transitions. As part of this work, for the first time in alkaline-earth metal dimers we have observed excited states with even J' that have 'f-parity', opposite to the previously known odd-J' 'e-parity' states.

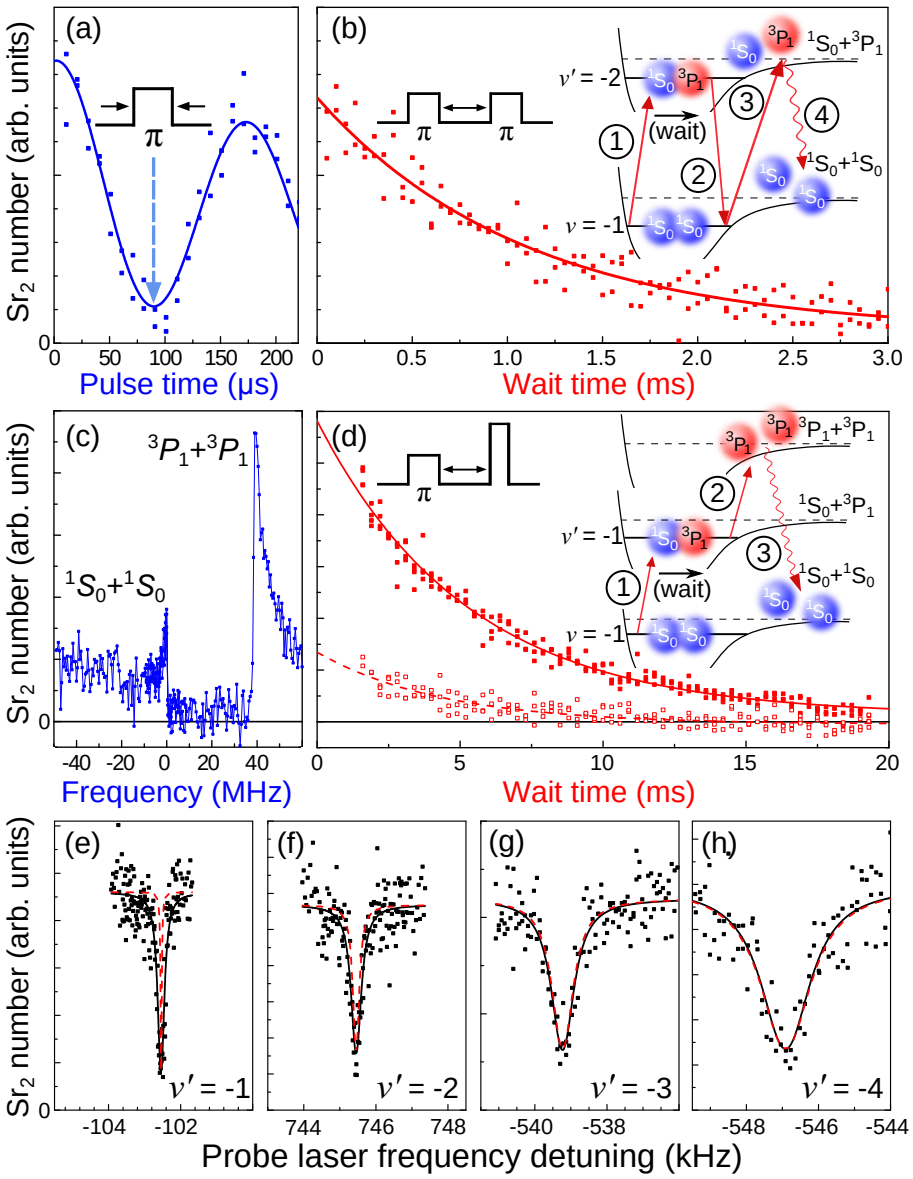

Figure 8: Direct and spectroscopic measurements of subradiant state lifetimes. For all the states, $J' = 1$. (a) Rabi oscillations between ground and excited gerade molecules that set the π-pulse lengths for lifetime measurements. (b) Excited-state population decay, fitted with an exponential curve. The cartoon illustrates the four-step measurement sequence used for all the gerade states but the least-bound one. (c) The least-bound gerade state is strongly coupled to the atomic continuum due to its large bond length $R \approx 130\ a_0$. The optical transition to the ${}^3P_1 + {}^3P_1$ continuum corresponds to the right-hand peak, and the ${}^1S_0 + {}^1S_0$ continuum to the left-hand oppositely facing peak. (d) Lifetime measurement of the least-bound state. The cartoon shows the simplified measurement sequence, using the right peak in panel (c). (e-h) Optical spectra of the four weakly bound $J' = 1$ subradiant states; the least-bound state is on the left. Dashed red lines indicate lineshapes deduced from direct lifetime measurements as in panels (b,d). Only the narrowest spectra are limited by technical broadening such as the laser linewidth. Graphics from Ref. [10].

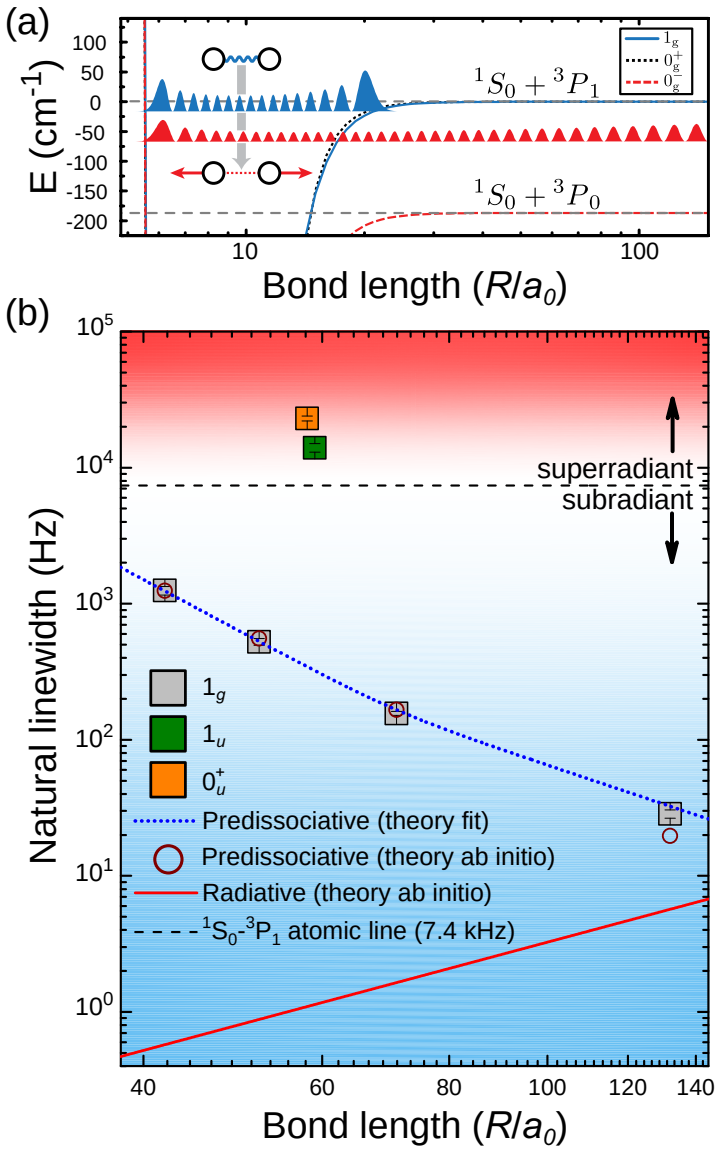

Figure 9: Natural linewidths of weakly bound subradiant and superradiant molecular states. (a) The dominant contribution to the natural lifetime of the long-range subradiant states is gyroscopic predissociation sensitive to short-range physics, as schematically shown here. (b) Four least-bound subradiant states of $^{88}Sr_2$ with the lowest angular momentum $J' = 1$ are measured, covering the range of bond lengths $R \sim$ 40-130 a_0. The threshold between superradiant and subradiant behavior is marked, as well as measurements of two representative superradiant states. Calculations of subradiant widths include both radiative and nonradiative contributions. The former scale as $\propto R^2$ (the line is ab initio theory), and the latter as the vibrational energy spacing (the line is theory fit to the data with a single scaling parameter; ab initio theory points are also shown). Graphics from Ref. [10].

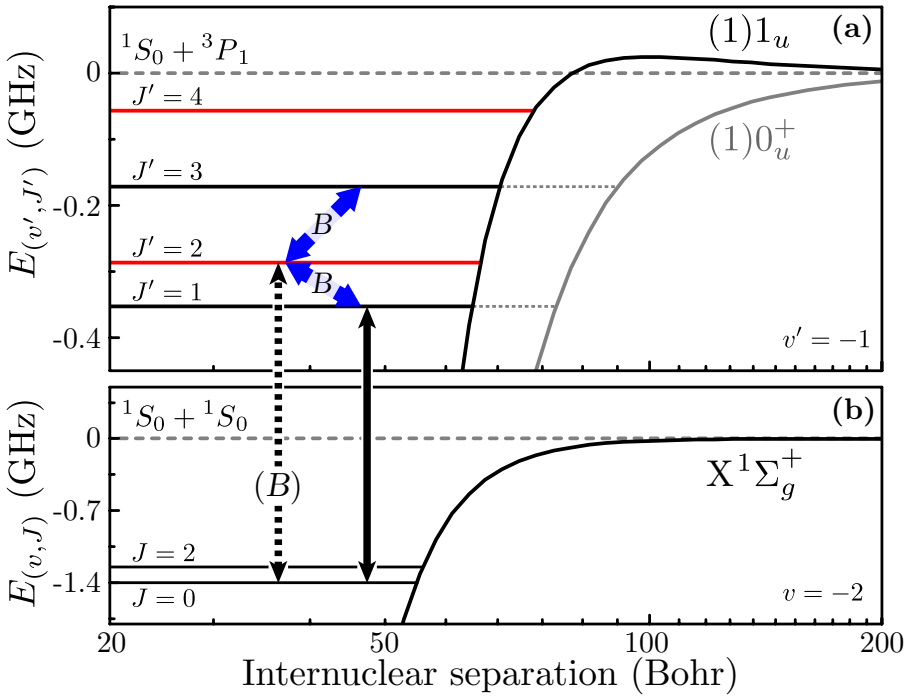

Figure 10: A magnetically enabled electric-dipole forbidden molecular transition. (a) Admixing of 1_u excited states by an applied static magnetic field B (slanted arrows). Nearby 0_u^+ states also admix but are omitted for clarity. States with odd J' are of both $1_u/0_u^+$ character (horizontal dashed lines) because of nonadiabatic Coriolis coupling [19]. (b) An optical transition from $J = 0$ to $J' = 2$ is electric-dipole forbidden (dashed vertical arrow), while to $J' = 1$ is allowed (solid vertical arrow). With an applied field, the forbidden transition becomes allowed because of admixing with the $J' = 1$ state. Graphics from Ref. [20].

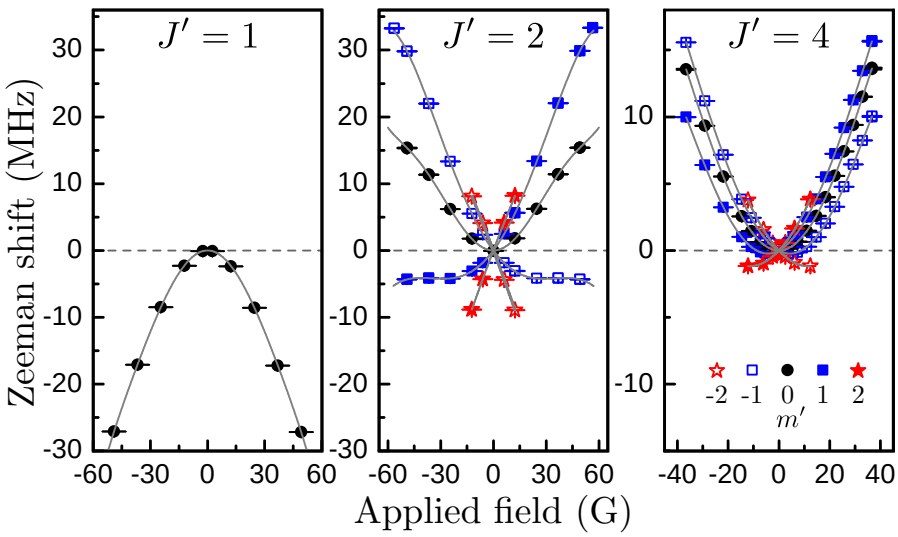

Figure 11: Highly nonlinear Zeeman shifts measured for the three $1_u(v' = -1, J')$ states shown in Fig. 12(a-d). The lines are polynomial fits with appropriate symmetry constraints, leading to magnetic shift coefficients up to the sixth order in field strength B. Graphics from Ref. [20].

Moreover, until now literature has been unclear on the possibility of even observing such states [21].

Enabling forbidden transitions with magnetic mixing has been previously successfully attempted for atomic lattice clocks [22]. With molecules, the technique potentially holds even larger promise, since nonlinear magnetic (Zeeman) shifts are orders of magnitude greater for the dense molecular level structure than for comparable atoms. Figure 11 shows highly nonlinear shifts that we precisely measured up the the 6th order in field strength B [20]. These shifts are apparent at modest fields of tens of gauss.

Figure 12 shows the results of optical transition strength tuning with modest magnetic fields. The strengths are referenced to the E1-allowed transition in Fig. 12(b), and $\Delta J \leq 3$ were accessed. Strength tuning over five orders of magnitude was achieved, as e.g. in Fig. 12(c). Figure 12(a) demonstrates constructive and destructive interferences of transition strengths for certain quantum numbers of the initial and final states [20].

An important component of this project's success is the remarkable agreement between experiment and theory shown in Figs. 11, 12. The agreement yields full confidence in the ab initio model used in conjunction with our molecular clock experiment [17, 23].

The unprecedented degree of transition strength tuning achievable in asymptotic Sr_2 molecules can be used to engineer even more precise molecular clocks. While subradiant states belonging to the 1_g excited molecular potential have been observed and studied (Sec. 3), the 0_g^+ states with the same $^1S_0 + ^3P_1$ asymptote have not yet been observed. Such states are expected to not suffer from predissociation (Fig. 9(a)), and thus provide optical molecular transitions with sub-hertz natural linewidths that could be strengthened by admixing neighboring 1_g subradiant states with our technique.

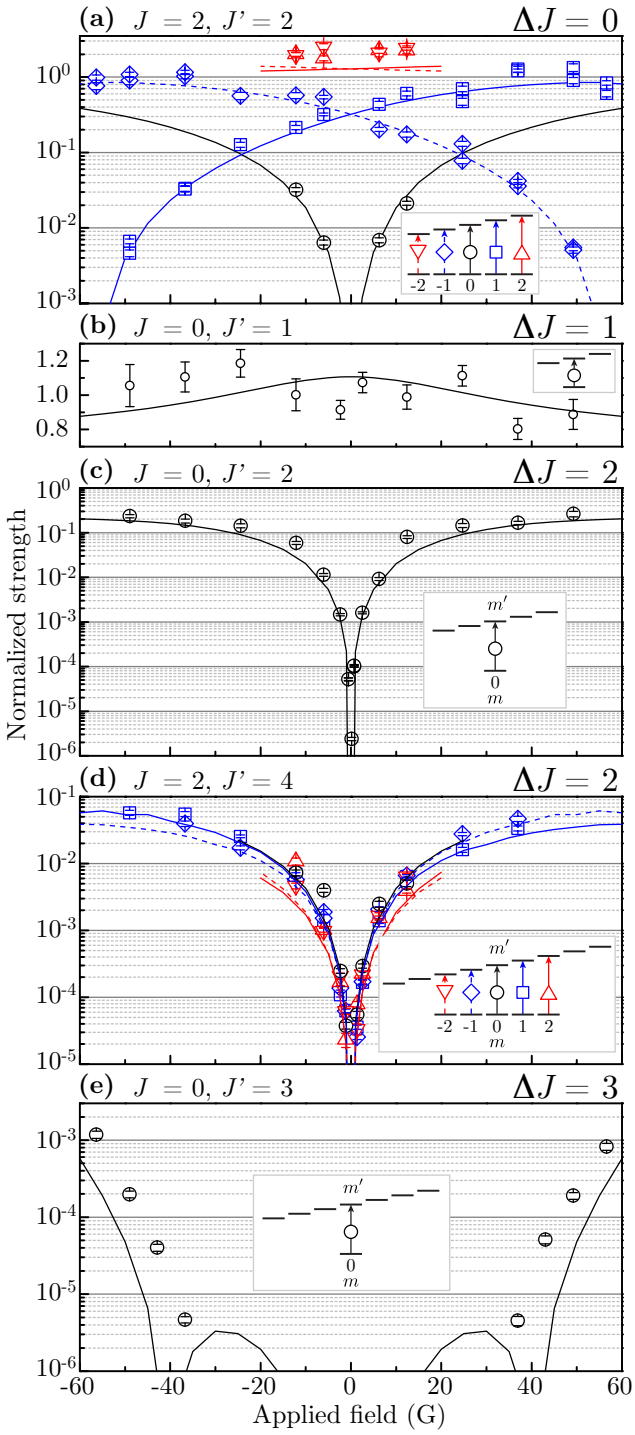

Figure 12: Magnetic control of molecular transitions between $X^1\Sigma_g^+(v = -2, J, m)$ ground states and $1_u(v' = -1, J', m')$ excited states for $J' = 1, 2, 4$ and $0_u^+(v' = -3, J', m')$ for $J' = 3$. Points are experimental values and curves are *ab initio* calculations. (a) An allowed transition with $\Delta J = 0$ has an 'accidentally' forbidden $m = m' = 0$ component that becomes allowed with field, and $m = m' = \pm 1$ components that show interference from admixing. (b) An allowed transition with $\Delta J = 1$ is mostly field-insensitive. Its average value is used to normalize the data. (c,d) Forbidden transitions with $\Delta J = 2$ and strengths that vary over five orders of magnitude to become comparable to allowed transitions. (e) A highly forbidden transition with $\Delta J = 3$ enabled by second-order admixing. Graphics from Ref. [20].

5 Anomalous magnetizability and measurements of nonadiabatic effects

As reported previously, the large nonlinear Zeeman shifts of weakly bound Sr_2 near the intercombination-line threshold were measured for a variety of states, and explained by considering nonadiabatic effects (Coriolis coupling) in weakly bound molecules [19, 20]. The linear shift coefficients yield the nonadiabatic mixing angles of the molecular wavefunctions, and thus provide a direct window into the phases and amplitudes of the wavefunctions. Furthermore, anomalously large quadratic shifts (or magnetic susceptibilities) are over a million-fold enhanced compared to those of free $^3P_1$ Sr atoms. The quadratic shifts were shown to increase roughly cubically with the size of the molecule, by adapting a simple model of magnetic susceptibility. The susceptibility is enhanced by the proximity of the weakly bound molecular states to the atomic continuum. The correct prediction of the quadratic and higher-order Zeeman shifts requires precise description of the continuum and bound levels with $\Delta J' = 0, \pm 1$; thus, these shifts provide a substantially more stringent test of the ab initio molecular model than the linear shifts alone.

6 Outlook

As evident from the prior sections, the Columbia molecular clock project has been (and continues to be) a success. We have built a reliable, technically complex, and unique experiment that combines ultracold molecule science with optical lattice clock techniques. It has allowed us to investigate physics that has been inaccessible thus far, and to overcome many exciting technical challenges such as state-insensitive trapping of molecules and ultracold thermometry. The work has also illuminated a path forward, in terms of engineering new ultraprecise optical molecular clocks as well as two-photon terahertz molecular clocks. The latter is poised to set more stringent laboratory limits on the stability of the electron-to-proton mass ratio [24, 25] and serve as a state-of-the-art probe for small mass-dependent forces at the nanometer scale [26]. As the starting point to the nanoscale force research, the abundance of spinless bosonic Sr isotopes suggests that fitting mass-dependent corrections to the ground-state Born-Oppenheimer interatomic potential [27] should extract a highly competitive constraint to new physics, and in addition will yield a new level of precision for measuring and calculating molecular vibrations.

Furthermore, we have opened a new research direction of ultracold molecular photodissociation. A glimpse of this process is illustrated in Fig. 13. It allows us to probe bound-to-free one- and two-photon molecular transitions with microkelvin resolution of the fragment energies. Photofragmentation has not been previously applied in the ultracold regime, and we are in the process of using it to directly and experimentally confirm the Wigner threshold law and to learn about the asymptotic regime of the continuum. This is particularly valuable for the atomic thresholds that are important for experiments but are not well understood theoretically, such as $^3P_1 + ^3P_1$ for alkaline-earth metals. In addition, ultracold photodissociation has direct applications in our future work of laser cooling diatomic hydrides and possibly producing ultracold, dilute hydrogen samples from such molecules.

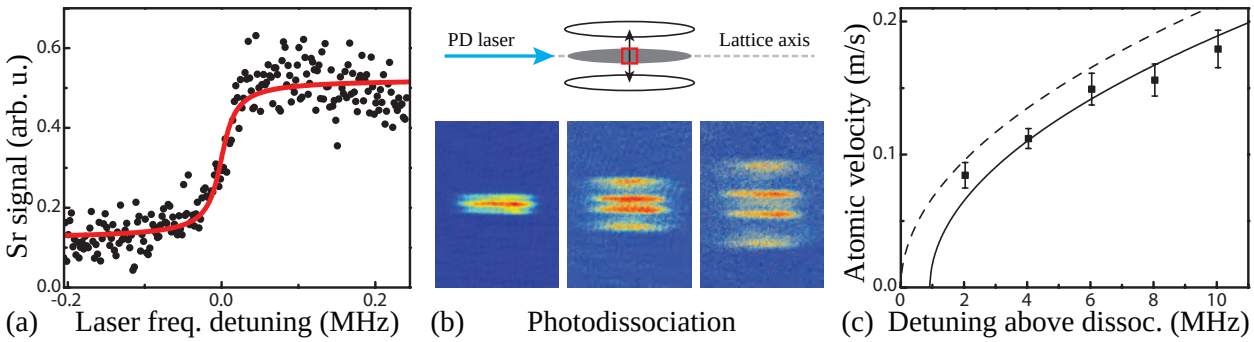

Figure 13: Intercombination-line molecular photodissociation. (a) A 'shelf' line shape obtained by optically exciting ground-state $X^1\Sigma_g^+(v = -2, J = 0)$ molecules to the excited-state $^1S_0 + {}^3P_1$ atomic continuum. The spectrum is fit with an inverse-tangent line shape characteristic of 2D photodissociation. (b) With increased detuning above the continuum, the resulting atoms have enough energy to escape the optical lattice. Viewed off-axis as sketched (top) and observed with absorption imaging (bottom), this occurs mainly along a preferred direction set by the photodissociation laser polarization. Two pairs of vertically split clouds appear in the successively delayed absorption images: an outer pair of faster atoms from $J = 2$ photodissociation, and an inner pair of slower atoms from $J = 0$ photodissociation. (c) The measured velocities of the atoms in the slower, inner clouds. The dashed curve is a speed limit from energy conservation. The solid curve is a fit to the data, offset by the lattice depth. Graphics from Ref. [12].

7 Education and outreach

The technological and scientific significance of the project was described in Secs (1-6). This work has also made a strong impact on education and training of the next generation of students and scientists. In the course of the work, the experiment supplied professional and scientific training to a research scientist, a postdoctoral researcher, three graduate students including a completed PhD degree, ten undergraduate students including a completed undergraduate thesis, and two high school students. The second PhD thesis on the molecular clock project is close to completion.

References

[1] M. McDonald, B. H. McGuyer, G. Z. Iwata, and T. Zelevinsky. Thermometry via light shifts in optical lattices. *Phys. Rev. Lett.*, 114:023001, 2015.

[2] D. Leibfried, R. Blatt, C. Monroe, and D. Wineland. Quantum dynamics of single trapped ions. *Rev. Mod. Phys.*, 75:281–324, 2003.

[3] Lincoln D. Carr, David DeMille, Roman V. Krems, and Jun Ye. Cold and ultracold molecules: science, technology and applications. *New J. Phys.*, 11:055049, 2009.

[4] Hidetoshi Katori. Optical lattice clocks and quantum metrology. *Nature Photon.*, 5:203, 2011.

[5] G. Reinaudi, C. B. Osborn, M. McDonald, S. Kotochigova, and T. Zelevinsky. Optical Production of Stable Ultracold $^{88}Sr_2$ Molecules. *Phys. Rev. Lett.*, 109:115303, 2012.

[6] T. Zelevinsky, M. M. Boyd, A. D. Ludlow, T. Ido, J. Ye, R. Ciuryło, P. Naidon, and P. S. Julienne. Narrow Line Photoassociation in an Optical Lattice. *Phys. Rev. Lett.*, 96:203201, 2006.

[7] Paul D. Lett, Richard N. Watts, Christoph I. Westbrook, William D. Phillips, Phillip L. Gould, and Harold J. Metcalf. Observation of Atoms Laser Cooled below the Doppler Limit. *Phys. Rev. Lett.*, 61:169, 1988.

[8] J. Ye, H. J. Kimble, and H. Katori. Quantum State Engineering and Precision Metrology Using State-Insensitive Light Traps. *Science*, 320:1734–1738, 2008.

[9] S. Blatt, J. W. Thomsen, G. K. Campbell, A. D. Ludlow, M. D. Swallows, M. J. Martin, M. M. Boyd, and J. Ye. Rabi spectroscopy and excitation inhomogeneity in a one-dimensional optical lattice clock. *Phys. Rev. A*, 80:052703, 2009.

[10] B. H. McGuyer, M. McDonald, G. Z. Iwata, M. G. Tarallo, W. Skomorowski, R. Moszynski, and T. Zelevinsky. Precise study of asymptotic physics with subradiant ultracold molecules. *Nature Phys.*, 11:32–36, 2015.

[11] D. C. McKay and B. DeMarco. Cooling in strongly correlated optical lattices: prospects and challenges. *Rep. Prog. Phys.*, 74:054401, 2011.

[12] B. H. McGuyer, M. McDonald, G. Z. Iwata, M. G. Tarallo, A. T. Grier, F. Apfelbeck, and T. Zelevinsky. High-precision spectroscopy of ultracold molecules in an optical lattice. *New J. Phys., accepted*, 2015.

[13] M. Gross and S. Haroche. Superradiance: An essay on the theory of collective spontaneous emission. *Phys. Rev.*, 93:301–396, 1982.

[14] R. G. DeVoe and R. G. Brewer. Observation of Superradiant and Subradiant Spontaneous Emission of Two Trapped Ions. *Phys. Rev. Lett.*, 76:2049–2052, 1996.

[15] Yosuke Takasu, Yutaka Saito, Yoshiro Takahashi, Mateusz Borkowski, Roman Ciuryło, and Paul S. Julienne. Controlled Production of Subradiant States of a Diatomic Molecule in an Optical Lattice. *Phys. Rev. Lett.*, 108:173002, 2012.

[16] Béatrice Bussery-Honvault and Robert Moszynski. *Ab initio* potential energy curves, transition dipole moments and spin−orbit coupling matrix elements for the first twenty states of the calcium dimer. *Mol. Phys.*, 104:2387–2402, 2006.

[17] Wojciech Skomorowski, Filip Pawłowski, Christiane P. Koch, and Robert Moszynski. Rovibrational dynamics of the strontium molecule in the $A^1\Sigma_u^+$, $c^3\Pi_u$, and $a^3\Sigma_u^+$ manifold from state-of-the-art *ab initio* calculations. *J. Chem. Phys.*, 136:194306, 2012.

[18] A. D. Ludlow, X. Huang, M. Notcutt, T. Zanon-Willette, S. M. Foreman, M. M. Boyd, S. Blatt, and J. Ye. Compact, thermal-noise limited optical cavity for diode laser stabilization at 1×10^{-15}. *Opt. Lett.*, 32:641–643, 2007.

[19] B. H. McGuyer, C. B. Osborn, M. McDonald, G. Reinaudi, W. Skomorowski, R. Moszynski, and T. Zelevinsky. Nonadiabatic Effects in Ultracold Molecules via Anomalous Linear and Quadratic Zeeman Shifts. *Phys. Rev. Lett.*, 111:243003, 2013.

[20] B. H. McGuyer, M. McDonald, G. Z. Iwata, W. Skomorowski, R. Moszynski, and T. Zelevinsky. Control of optical transitions with magnetic fields in weakly bound molecules. *arXiv:1503.05946*, 2015.

[21] O. Allard, St. Falke, A. Pashov, O. Dulieu, H. Knöckel, and E. Tiemann. Study of coupled states for the $(4s^2)^1S + (4s4p)^3P$ asymptote of Ca_2^*. *Eur. Phys. J. D*, 35:483–497, 2005.

[22] Z. W. Barber, C. W. Hoyt, C. W. Oates, L. Hollberg, A. V. Taichenachev, and V. I. Yudin. Direct Excitation of the Forbidden Clock Transition in Neutral ^{174}Yb Atoms Confined to an Optical Lattice. *Phys. Rev. Lett.*, 96:083002, 2006.

[23] Mateusz Borkowski, Piotr Morzyński, Roman Ciuryło, Paul S. Julienne, Mi Yan, Brian J. DeSalvo, and T. C. Killian. Mass scaling and nonadiabatic effects in photoassociation spectroscopy of ultracold strontium atoms. *Phys. Rev. A*, 90:032713, 2014.

[24] T. Zelevinsky, S. Kotochigova, and J. Ye. Precision Test of Mass-Ratio Variations with Lattice-Confined Ultracold Molecules. *Phys. Rev. Lett.*, 100:043201, 2008.

[25] A. Shelkovnikov, R. J. Butcher, C. Chardonnet, and A. Amy-Klein. Stability of the Proton-to-Electron Mass Ratio. *Phys. Rev. Lett.*, 100:150801, 2008.

[26] E. G. Adelberger, B. R. Heckel, and A. E. Nelson. Tests of the gravitational inverse-square law. *Annu. Rev. Nucl. Part. Sci.*, 53:77, 2003.

[27] M. Puchalski, D. Kędziera, and K. Pachucki. Ionization potential for excited S states of the lithium atom. *Phys. Rev. A*, 82:062509, 2010.